remote sensing

IMPACT FACTOR 4.2

CITESCORE 8.3

Article

# Evaluation of Spectroscopy and Methodological Pre-Treatments to Estimate Soil Nutrients in the Vineyard

Marta Rodríguez-Febereiro, Jorge Dafonte, María Fandiño, Javier J. Cancela and José Ramón Rodríguez-Pérez

MDPI

https://doi.org/10.3390/rs14061326

*remote sensing*

*Article*

# Evaluation of Spectroscopy and Methodological Pre-Treatments to Estimate Soil Nutrients in the Vineyard

**Marta Rodríguez-Febereiro [1], Jorge Dafonte [1], María Fandiño [1], Javier J. Cancela [1,*] and José Ramón Rodríguez-Pérez [2]**

[1] GI-1716, Proyectos y Planificación, Departamento Ingeniería Agroforestal, Escola Politécnica Superior de Enxeñaría, Universidade de Santiago de Compostela, Rúa Benigno Ledo s/n, 27002 Lugo, Spain; martarodriguez.fernandez@usc.es (M.R.-F.); jorge.dafonte@usc.es (J.D.); maria.fandino@usc.es (M.F.)

[2] Grupo de Investigación en Geomática e Ingeniería Cartográfica (GEOINCA), Universidad de León, Avenida de Astorga s/n, 24401 León, Spain; jr.rodriguez@unileon.es

* Correspondence: javierjose.cancela@usc.es

**Abstract:** The characterization of vineyard soil is a key issue for crop management, which directly affects the quality and yield of grapes. However, traditional laboratory analysis of soil properties is tedious and both time and cost consuming, which is not suitable for precision viticulture. For this reason, a fast and convenient soil characterization technique is needed for soil quality assessment and precision soil management. Here, spectroscopy appears as a suitable alternative to assist laboratory analysis. This work focuses on estimating soil properties by spectroscopy. Our study was carried out using 96 soil samples collected from three vineyards in Rias Baixas Designation of Origen (Galicia, Spain). The soils that were characterized include nitrogen (N), organic matter (OM) and clay content (Clay). The presented work compared two regression techniques (partial least squares (PLSR) and random forest (RF)) and four spectral ranges: visible—VIS (350–700 nm), near infrared—NIR (701–1000 nm), short wave infrared—SWIR (1001–2500 nm) and VIS-NIR-SWIR (350–2500 nm) in order to identify the more suitable prediction models. Moreover, the effect of pre-treatments in reflectance data (smoothing Svitzky–Golay, SG, baseline normalization, BN, first derivative, FD, standard normal variate, SNV, logarithm of 1/reflectance or spectroscopy (SP) and detrending, SNV-D) was evaluated. Finally, continuous maps of the soil properties were created based on estimated values of regression models. Our results identified PLSR as the best regression technique, with less computation time than RF. The data improved after applying transformation in reflectance data, with the best results from spectroscopy pre-treatment (logarithm of 1/Reflectance). PLSR performances have obtained determination coefficients ($R^2$) of 0.69, 0.73 and 0.52 for nitrogen, organic matter, and clay, respectively, with acceptable accuracy (RMSE: 0.03, 1.06 and 2.90 %) in a short time. Furthermore, the mapping of soil vineyards generates information of high interest for the precision viticulture management, as well as a comparison between the methodologies used.

**Keywords:** organic matter; VIS; NIR; precision viticulture; PLSR; random forest

**Citation:** Rodríguez-Febereiro, M.; Dafonte, J.; Fandiño, M.; Cancela, J.J.; Rodríguez-Pérez, J.R. Evaluation of Spectroscopy and Methodological Pre-Treatments to Estimate Soil Nutrients in the Vineyard. *Remote Sens.* **2022**, *14*, 1326. https://doi.org/10.3390/rs14061326

Academic Editor: Dominique Arrouays

Received: 29 January 2022
Accepted: 7 March 2022
Published: 9 March 2022

## 1. Introduction

The soil properties in a vineyard are a key factor to consider for practicing precision viticulture, which directly influences the development of the plants, as well as the production, which implies more friendly and sustainable practices in a modern viticulture [1].

Organic matter (OM) and nitrogen (N) play substantial roles in soil chemical, physical and biological processes. They are also a good indicator of fertility, productivity and nutrient availability [2]. Maintaining soil fertility is the basis of all forms of sustainable soil use and requires preservation of OM, physical properties and nutrient levels. In most cases, the leading factor involved in soil fertility is nutrient status.

Acidic soils (Galicia, Spain) generally imply a high OM content in the soil [3]. The variability and change in the soil characteristics in the vineyards have a direct impact on plant development, as well as on the wine characteristics, influenced by the different soil properties that the vineyard may present [4].

Thus, in order to characterize its spatial variability, it is essential to collect and analyze a large number of samples, which is time consuming and expensive using traditional soil analysis methods [5]. Therefore, it is necessary to find a cost-effective approach that is suitable and reliable to estimate the spatial distribution of soil nutrients in the vineyard. Advances of soil spectroscopy have a significant impact in many soil science fields; for instance, quantitative spectroscopy is being used in the evaluation and monitoring of soil quality, and soil function, soil fertility, soil degradation, soil mapping, classification and soil contamination are nowadays examined using hyperspectral remote sensing, enlarging the soil spectroscopy into a spatial domain [6]. In recent decades, numerous studies have used Digital Soil Map (DSM) approaches to predict the spatial distribution of soil classes or properties that help the winegrower to visualize the heterogeneity of their vineyard to apply precision viticulture that allows them to improve the vineyard management [7]. However, to be more efficient, spectroscopy has the potential to provide inexpensive, fast and robust quantitative characterization of the different physicochemical properties [8].

Spectral information is obtained from the energy reflected as the interaction with the constituents of the object. This energy results from the interaction of four factors: organic matter content, soil moisture, minerals and texture [9]. Spectral data are usually pre-processed through approaches to accentuate features and remove signal noise [10]. The soil spectra that are processed facilitate identification, and the accuracy of mineral soil prediction is greatly improved through the use of various pre-processing methods. Previous studies have used pre-processing methods for spectra analysis and their relations with soil properties [11].

Several studies have focused on measuring soil properties using spectroscopy methodology, analyzing the effect of the spectra reflectance affected by soil properties [12] or using the reflectance to predict total organic C, N and moisture content [13]. Other authors focused on the reflectance spectrum in the VIS-NIR-SWIR regions in the mechanism of soil–radiation interactions [14] or to obtain a polynomial function to characterize the organic matter content between 400 and 1600 nm [15]. Other applications are the study of different spectral patterns between 400 and 2500 nm to determine organic matter, iron, silt, sand and clay content [16] and to determine the spectral information that can be used for soil classification because they present statistically significant differences between spectral profiles [17]. Similar studies have been carried out; however, the analysis of this application on the cultivation of the vineyard, in a wine-growing area such as the study, in which there are not data at the intra-plot level, is studied in this work in a methodological way to obtain the flowchart to apply in subsequent studies [18].

The main goal of this study is to establish a flowchart for the treatment of spectral data, which allows us to obtain a good methodology that allows for the use of spectroscopy as an efficient method for the estimation of soil properties, as well as to generate maps of the variability of the soil properties, which allow the winegrowers to apply effective precision viticulture.

## 2. Materials and Methods

### 2.1. Description of the Study Areas

The study was conducted in three different locations/plots (Northwest of Spain, Figure 1), within the 'Rías Baixas' Designation of Origin (DO): (A) Lobeira (42°34′7.47″N, 8°45′17.37″W; 119 m.a.s.l.; 7.98 ha); (B) Monteveiga (42°45′6″N, 8°28′10″W; 131 m.a.s.l.; 12.04 ha); (C) Ribadulla vineyards (42°46′13″N, 8°24′40″W; 66 m.a.s.l.; 9.36 ha). the three vineyards were planted in 2004, with *Vitis vinifera* cv. 'Albariño' and a 2.50 × 3 m vine by row spacing.

The trellis system consisted of a thumb rod trained for vertical shoot positioning; the rootstock was 110 Ritcher, and the vineyards utilize drip irrigation throughout the cultivated areas. The soil at this site is developed upon granite bedrocks and is classified as an Anthrosol (IUSS Working Group WRB, 2015, n.d.). The geography of Rias Baixas includes a set of heterogeneous inlets that are considered according to the hydrodynamic and sedimentological characteristics, which are grouped according to the wine sub-zone that shares geographic characteristics. In this case, two of the vineyards are located under the 'Ribeira do Ulla' sub-zone (Monteveiga and Ribadulla), with a main geological class being migmatite (metamorphic boulder), and the Lobeira plot is located under the ´Val do Salnés´ subzone, in which the granodiorite boulder predominates. The geological characteristics of each vineyard are different and can be visualized using IGME maps (IGME. Geological and Mining Institute of Spain. Web Site, n.d.).

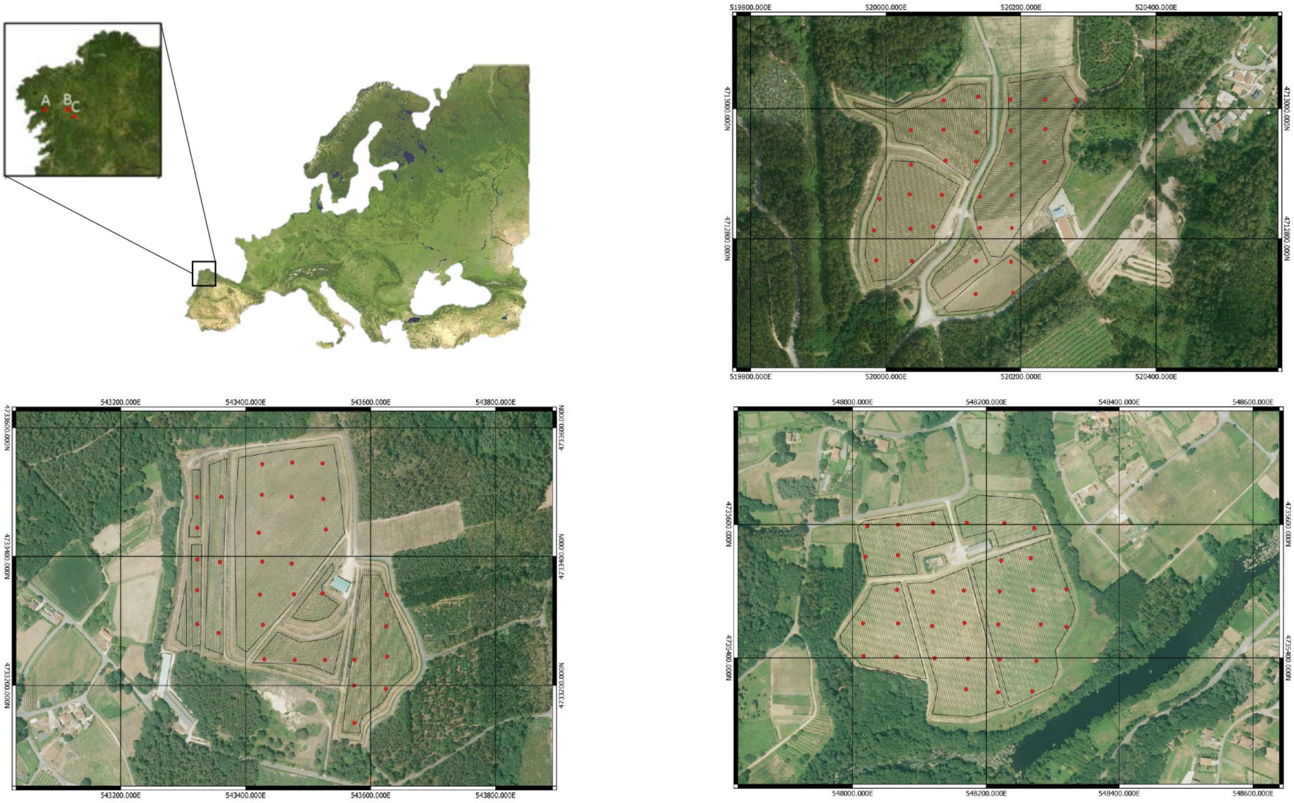

**Figure 1.** Study area locations—Galicia (Spain): (**A**) Lobeira (Vilagarcía de Arousa), (**B**) Monteveiga (Vedra) and (**C**) Ribadulla (Vedra). Soil sampling points are shown as red points.

## *2.2. Soil Sampling and Laboratory Analysis*

A total of 96 soil samples were collected from the three plots, 32 samples per vineyard. At each site, samples were taken from the surface horizon (0–40 cm depth) in a regular grid (separated by 30 × 30 m) in the month of June 2020 (Figure 1). The same number and samples were used for the classical laboratory analysis and for the spectroscopy analysis. A GNSS-RTK receiver (Hi-Target V200, Guangzhou, China) was used to georeference the measurement points.

The samples collected were oven dried (60 °C) and sieved at 2.00 mm to separate the fine soil fraction, the physical–chemical analysis were determined according to standard methods [19]. The soil properties analyzed in this case were as follows: clay content, of interest in terms of the water retention [20], and N and OM content, fundamental parameters in terms of the vineyard fertility, which directly affect the nutrition of the plants and therefore their vegetative development and production [21].

Laboratory analyses were carried out for clay content based on the method from [22]. Total organic carbon (C) and nitrogen (N) contents were measured with an elemental analyzer (TruSpec-CHNS, LECO Corporation, St. Joseph, MI, USA). Organic matter (OM) was computed from the carbon content [23] using Equation (1).

$$\text{OM }(\%) = \text{C }(\%) \times 1.724 \tag{1}$$

### *2.3. Spectral Data Acquisition and Pre-Processing*

The spectral reflectance of the soil samples was measured under laboratory conditions using a portable spectroradiometer, ASD FieldSpec®4 Standard-Res (Analytical Spectral Devices, Inc., Boulder, CO, USA). This equipment captures radiance or reflectance values from 350 nm to 2500 nm (spectral resolution of 10 nm) and collects light passively with a fiber optic cable.

To manage the process of reflectance measurements, the RMS3TM v.6.3.0 software (Boulder, CO, USA) was used. The protocol for capturing reflectance was the following: (1) system optimization, (2) sensor calibration by the white panel (Spectralon®, North Sutton, NH, USA) and (3) spectral signature measurement of each soil sample. Three reflectance values were taken at three different positions of the sample in order to obtain a more representative spectral signature of each soil sample.

The raw spectral data were processed: first, averages of the three measurements were calculated for each soil sample; second, an exploratory statistical analysis was carried out to detect possible outliers (any anomalous signature was detected). Then, pre-processing techniques were applied in order to reduce noise or unwanted signal artifacts and to highlight the spectral features related to the studied soil properties [24].

The pre-processing consisted of applying the transformation to raw spectral data. We applied six transformations: signal smoothing by Savitzky-Golay (SG), baseline normalization (BN), first derivative (FD), standard normal variate (SNV), logarithm of 1/reflectance or spectroscopy (SP) and standard normal variate and detrending (SNV-D). All selected transformations are frequently used and defined in the literature [11] and were applied to try to improve the subsequent exploratory analysis and classification and calibration models [25]. Transformations were calculated using the software Unscrambler® X 11 (CAMO Software Inc., Woodbridge, Norway), whose calculation procedures are detailed in [26].

Finally, four different spectral subsets were defined regarding the wavelength ranges used as prediction variables: VIS: (350–700 nm), NIR: (701–1000 nm), SWIR: (1000–2500 nm) and full range: (350–2500 nm).

### *2.4. Prediction Models*

To predict the soil data, several techniques were developed in the study. Figure 2 includes the flow chart with the process followed from soil samples performing the classic laboratory analyses and spectroscopy measurements, in which different pretreatments have been studied to finally map the results comparing both methods, which is explained in detail in the following sections.

#### 2.4.1. Regression Analysis: Calibration and Validation

The soil properties (predicted variables) were estimated from the spectral data (predictor variables) by partial least square regression (PLSR) and random forest (RF). For both regression techniques, several models were fitted using the four spectral subsets of raw and transformed reflectance. These transformations were carried out in order to compare and identify which was more suitable for predictions of soil properties (Figure 2).

Two subsets of soil were randomly defined with an equal distribution between the three study fields: one for training (*n* = 63; 21 samples per plot) and the other one for validation (*n* = 33; 11 samples per plot).

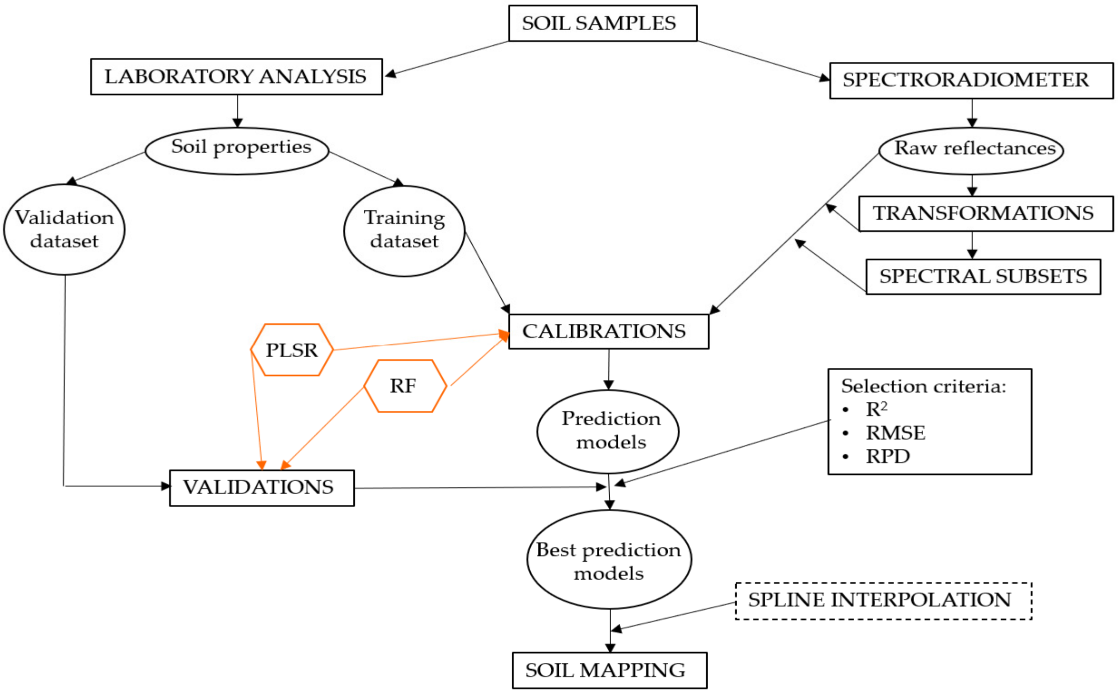

**Figure 2.** Flowchart of the methodology used: random forest (RF) and partial least square regression (PLSR).

### 2.4.2. Partial Least-Squares Regression (PLSR)

PLSR is a widespread modeling technique used in chemometrics and is commonly used for quantitative spectral analysis. The PLSR algorithm selects successive orthogonal factors that maximize the covariance between predictors and response variables [27]. The CV (cross-validation) method is often preferred to assess PLSR models for datasets with fewer than 50 samples [28–30]; however, we validated the calibrated models using an independent dataset. All PLSR analyses were performed using the Unscrambler® v. 11 (CAMO Analytics AS, Oslo, Norway).

### 2.4.3. Random Forest (RF)

Random forest (RF) is a nonparametric and ensemble model based on a regression tree algorithm [31]. The total results of all single trees are gathered to build a singular prediction. Parameters of the final model are selected by voting or averaging the value of the parameter in all calculated models [32]. In addition, RF is capable of ranking variables according to their relative importance for prediction based on the regression prediction error. The number of trees and the number of variables used at each split when building the tree are the most important parameters to tune in RF models [33].

In this study, the RF model was calculated using the R package “RandomForest” to assess the performance of the models with the same spectral data [34]. RF has been applied as a regression technique here. We used two approaches: the first approach (RF) was to apply the random forest method to the reflectance data and the transformed reflectance; the second approach (PC-RF) was to apply the principal components method (using four principal components), and on these principal components we used the method of random forest.

### 2.4.4. Statistics Estimating Model Performance

The performance of the models was evaluated using the following indicators to determine predictive qualities: the coefficient of determination ($R^2$), the root-mean-square error (RMSE), the standard error of prediction (SEP), the residual prediction deviation

(RPD) and the number of PLS factors [35]. Our criteria to select the best prediction models were highest $R^2$, lowest standard error (SEP) and highest RPD.

$R^2$ (Equation (2)) was used to assess the precision of the models:

$$R^2 = 1 - \frac{\sum\left(Y_i - Y'_i\right)^2}{\sum\left(Y_i - Y'\right)^2} \tag{2}$$

The RMSE and SEP were used to reflect the inaccuracy of the prediction models (Equations (3) and (4), respectively).

$$\mathrm{RMSE} = \sqrt{\frac{1}{n}\sum\left(Y_i - Y'_i\right)^2} \tag{3}$$

$$\mathrm{SEP} = \sqrt{\frac{\sum\left(Y_i - Y'_i\right)^2}{n-1}} \tag{4}$$

where $n$ is the number of samples, $Y_i$ is the observed value for the sample and $Y'_i$ is the predicted value for the sample.

RPD (Equation (4)) was calculated to assess the predictive ability of the VIS-NIR-SWIR prediction models.

$$\mathrm{RPD} = \frac{\mathrm{SD}}{\mathrm{RMSE}} \tag{5}$$

where SD is the standard deviation of the variable's reference values.

While RMSE and SEP use the same measurement units as the variable, the $R^2$ and RPD values are dimensionless so that they can be compared similarly between models for different properties. Higher values for the RPD indicate more accurate models. The RMSE should be lower than the SD, and the RPD should ideally be four or higher. The number of PLS factors is an indicator of the potential effectiveness of the calibration. In practice, most successful PLSR calibration equations indicate no more than six to eight factors. If the system uses 12–15 factors, this usually indicates some uncertainty in the computation [36].

### 2.5. Mapping for Soil Characterization

Characterization of vineyards soils from data captured by spectroscopy techniques is a very useful tool for vineyard management, which allows for the analysis of the state and of the behavior of the vineyard [37].

Mapping has been carried out by thin-plate splines (TPS) (Figure 2), also referred to as "minimum curvature" [38], which are implemented in the R "fields" package [39]; this is a quick way to see the distribution of a variable in space as a surface with an empirical method that adjusts locally to the data. In this method, there is no internal measure of prediction error, which is because there is no knowledge of the target variable's spatial structure, which is fitting a surface (as in the trend surface) but adjusting to local observations. This method is not "geostatistical" in the sense that there is no assumed model, other than the requirement that the fitted surface be in some sense "smooth". It fits a regional trend with local variations from the trend dependent on the observations [40].

The general method is to minimize the residual sum of squares (RSS) of the fitted function, subject to a constraint that the function be "smooth" in some sense; this is expressed by a roughness penalty or smoothing parameter (λ), which balances the fit to the observations with smoothness. This parameter was fitted by Generalized Cross-Validation (GCV) with the "fields" packages in R.

Previous studies in spectroscopy methodology allowed for mapping the plots with the variables of interest, which provides the farmer with information of high interest, to visualize the effects of fertilization and the performance of a precise agriculture by applying nutrients according to the needs required for the vineyards [41,42].

In this case, maps have been made in relation to the contents of the studied elements (N, OM and clay) in three ways: (1) using the complete dataset from laboratory analysis (32 data points per plot), (2) using the dataset estimated by PLSR with spectroscopy transformation (21 per plot, calibration data) and (3) difference of the estimation in both methodologies.

## 3. Results and Discussion

The basic statistics of the variables show, in global terms, that the Ribadulla plot had the lowest values of N and OM, but the highest average clay content. Conversely, Monteveiga plots obtained the highest values of N and OM, with Lobeira in an intermediate position. The results show a wide range of data for the three variables studied, with a low standard deviation (Table 1).

**Table 1.** Basic statistics for the soil samples data set ($n = 96$, 32 per plot). Results of laboratory analysis for N, OM and clay contents.

| | **N (%)** | **OM (%)** | **Clay (%)** |
|---|---|---|---|
| **Plot** | | **Mean** | |
| Lobeira | 0.20 | 4.28 | 21.01 |
| Monteveiga | 0.23 | 6.31 | 16.20 |
| Ribadulla | 0.13 | 2.57 | 22.94 |
| | | Maximum | |
| Lobeira | 0.32 | 7.57 | 29.30 |
| Monteveiga | 0.39 | 11.05 | 19.53 |
| Ribadulla | 0.26 | 6.07 | 30.86 |
| | | Minimum | |
| Lobeira | 0.11 | 2.07 | 15.51 |
| Monteveiga | 0.14 | 3.57 | 13.82 |
| Ribadulla | 0.06 | 1.01 | 15.58 |
| | | Standard deviation | |
| Lobeira | 0.05 | 1.20 | 3.59 |
| Monteveiga | 0.06 | 1.62 | 1.48 |
| Ribadulla | 0.05 | 1.29 | 3.71 |

### *3.1. Spectral Signatures and Main Variables*

The methodology used in the present work allowed for us to capture the spectral signatures of the 96 samples from the three plots under study (Figure 3).

The spectra of all the soils were similar, with minor features in the visible and near-infrared ranges of the spectrum. Due to the broad and overlapping bands, VIS-NIR spectra contained fewer absorption than the SWIR range, which can be more difficult to interpret [43]. According to the literature, these wavelengths are where the concentrations of elements in the soil are located [44]. In the same way as [45], the spectra showed absorption bands at wavelengths between 1400 and 2500 nm, related to the chemical bonds of the soil elements.

From the set of variables studied, the elements N, OM and clay presented the best relationships with the full wavelength reflectance (with $R^2$ values greater than 0.5 in all of the methodologies studied).

### *3.2. Partial Least-Squares Regression (PLSR) and Random Forest (RF) Analysis*

The results obtained from the processing of the variables (N, OM and clay), show how, in the methodologies used, the correlations depend on the data processing technique. Results using all the spectral ranges for RF demonstrated that models based on raw data improved determination coefficients ($R^2$) and reduced the estimation errors (RMSE) in comparison with the principal components models, despite having a higher computation time. For this reason, data without principal components were used (Table 2).

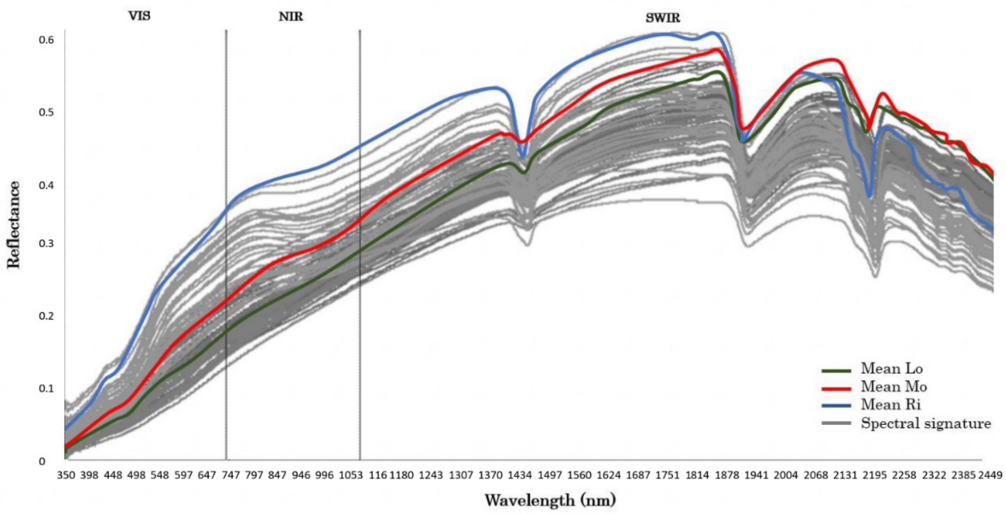

**Figure 3.** Spectral signatures of the 96 analyzed soil samples (spectral signature), and average spectral signatures of Lobeira (Mean Lo), Monteveiga (Mean Mo) and Ribadulla (Mean Ri).

**Table 2.** Statistics of random forest regressions using no transformed spectral data (RF) and calculating previously principal components (PC-RF).

| | **RF** | | **PC-RF** | |
|---|---|---|---|---|
| | **$R^2$** | **RMSE** | **$R^2$** | **RMSE** |
| N | 0.57 | 0.04 | 0.49 | 0.04 |
| OM | 0.68 | 1.18 | 0.59 | 1.34 |
| Clay | 0.50 | 2.91 | 0.51 | 0.76 |

R2 (coefficient of determination); RMSE (root-mean-square error).

Table 3 shows the data obtained from the processing with PLSR and RF (applied to the reflectance data). Most of the best correlations were captured in the SWIR and NIR range, and the highest correlation observed was in the OM content ($R^2$ = 0.84).

However, if we analyze the factors that define the models studied, a simpler model can be observed with the smallest errors between the predicted and observed values (RMSE), as well as typical validation error (SEP), RPD error and a reasonable number of factors. The calibration errors obtained are within the ranges that define robust prediction models, as well as RPD values (within the range 1.4–2.0), as established by the authors [46,47].

Other authors, who have studied the results obtained in the different wavelength ranges, obtain the best results when these are captured in the visible and near-infrared (VIS and NIR) range [48], as well as the study of soil properties with predictive variables that present a good correlation in the SWIR wavelength bands [49].

Regarding the methodology used for prediction of the soil variables, the PLSR was slightly higher in $R^2$ than RF. Other studies compared the methodologies used with more calibration variables for soil parameters, such as in terms of exchangeable cations in precision agriculture, with the results in the data obtained with the PLSR adjustment models being better than using other methodologies [50].

One method used to evaluate the spectral response for a soil property is to study the relationship between wavelength and the weighted regression coefficients values of the soil property. In Figure 4, N content had similar responses, but the response of the clay content was unique. N is the main element in soil, where OM and N are highly correlated. In contrast, clay content had a unique response.

These same patterns are contrasted in the research by [51], in which the behavior of C and N in vineyard agroecosystems was studied, with spectral signatures similar to those obtained in Galician soils.

**Table 3.** Statistics of PLSR and RF regression models using the four spectral subsets as prediction variables.

| | **PLSR** | | | | | **RF** | | | |
|---|---|---|---|---|---|---|---|---|---|
| | Nitrogen | | | | | Nitrogen | | | |
| | $R^2$ | RMSE | SEP | RPD | F | $R^2$ | RMSE | SEP | RPD |
| All r. | 0.53 | 0.04 | 0.04 | 1.64 | 3 | 0.57 | 0.04 | 0.04 | 1.49 |
| VIS | 0.53 | 0.04 | 0.04 | 1.64 | 1 | 0.61 | 0.04 | 0.04 | 1.58 |
| NIR | 0.50 | 0.04 | 0.04 | 1.67 | 1 | 0.53 | 0.04 | 0.04 | 1.41 |
| SWIR | 0.53 | 0.04 | 0.04 | 1.64 | 4 | 0.43 | 0.05 | 0.05 | 1.27 |
| | Organic matter | | | | | Organic matter | | | |
| | $R^2$ | RMSE | SEP | RPD | F | $R^2$ | RMS | SEP | RPD |
| All r. | 0.61 | 1.29 | 1.28 | 1.62 | 4 | 0.68 | 1.18 | 1.20 | 1.74 |
| VIS | 0.57 | 1.35 | 1.36 | 1.66 | 1 | 0.68 | 1.16 | 1.18 | 1.77 |
| NIR | 0.84 | 0.79 | 0.80 | 1.39 | 6 | 0.57 | 1.36 | 1.38 | 1.51 |
| SWIR | 0.65 | 1.22 | 1.22 | 1.59 | 7 | 0.53 | 1.44 | 1.46 | 1.43 |
| | Clay | | | | | Clay | | | |
| | $R^2$ | RMSE | SEP | RPD | F | $R^2$ | RMSE | SEP | RPD |
| All r. | 0.68 | 2.34 | 2.31 | 1.55 | 7 | 0.50 | 2.91 | 2.95 | 1.41 |
| VIS | 0.37 | 3.34 | 3.31 | 1.79 | 3 | 0.51 | 3.01 | 3.06 | 1.36 |
| NIR | 0.67 | 2.34 | 2.33 | 1.55 | 5 | 0.56 | 2.70 | 2.74 | 1.51 |
| SWIR | 0.68 | 2.33 | 2.35 | 1.56 | 7 | 0.47 | 3.00 | 3.05 | 1.36 |

$R^2$ (coefficient of determination); RMSE (root-mean-square error); SEP (standard error); SD (standard error of reference data); RPD (residual prediction deviation); F (Number of model factors). VIS: (350–700 nm), NIR: (701–1000 nm), SWIR: (1000–2500 nm) and All r.: (350–2500 nm).

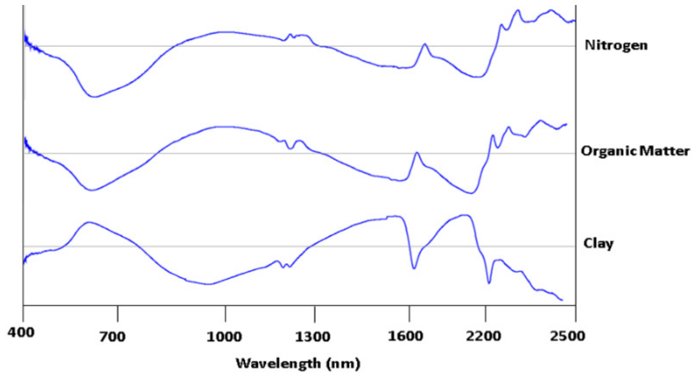

**Figure 4.** Weighted regression coefficient distribution over the spectral range obtained from PLSR. Black dotted lines represent zero correlation and have an offset by 1.0 units for clarity of presentation.

### *3.3. Transformations*

With the spectral pre-treatments defined, it was observed how the transformations that were carried out with signal smoothing (SG) maintain the $R^2$ values but increase the number of factors used in the model. Baseline normalization (BN) maintains the range of values of $R^2$ with a slight reduction in the value, improving the number of factors. The first derivative (FD) slightly lowers the value of $R^2$, but it significantly reduces the number of factors. Standard normal variate (SNV) keeps the $R^2$ values slightly lower and reduces the number of factors used. Finally, spectroscopy (SP) slightly increases the value of $R^2$ and reduces the number of factors, being therefore the transformation and correction of data that provides the best results, improving the prediction model used, except for the clay (Table 4).

However, several authors [52–54] note the benefit of transforming spectra before further analyses and determined that PLRS is a powerful regression technique that uses the full spectral range and thus finds the necessary information in all kinds of spectra. RF is another good tool that improves the correlations according to the wave range that is analyzed.

Furthermore, authors that studied different spectral ranges [55] have determined that pre-treatment might emphasize the information in all spectral data, so transformations that enhance spectral features generally have little impact on the visible and beginning of the NIR region because absorption features in this region are very broad. In our case, most of the best correlations were determined in the SWIR and NIR range, with which the studied spectral pre-treatments were defined.

Authors such as [56] that study soil fertility also obtained good values with FD and SG transformations. However, the soil analyzed carried out in agricultural plots by [57] found that the SG and SNV transformations were the ones that best fit the results obtained from the spectral signatures of the soil samples.

**Table 4.** Statistics of PLSR and RF regression models using the different transformations of spectral data as prediction variables. Transformations were applied to full spectral range (350–2500 nm).

| **PLSR** | | | | | | **RF** | | | |
|---|---|---|---|---|---|---|---|---|---|
| No transformation (NT) | | | | | | | | | |
| Variable | $R^2$ | RMSE | SEP | RPD | F | $R^2$ | RMSE | SEP | RPD |
| N | 0.53 | 0.04 | 0.04 | 1.64 | 3 | 0.57 | 0.04 | 0.04 | 1.49 |
| OM | 0.66 | 1.29 | 1.28 | 1.62 | 4 | 0.68 | 1.18 | 1.20 | 1.74 |
| Clay | 0.68 | 2.34 | 2.31 | 1.55 | 7 | 0.50 | 2.91 | 2.95 | 1.41 |
| Signal smoothing by Savitzky-Golay (SG) | | | | | | | | | |
| Variable | $R^2$ | RMSE | SEP | RPD | F | $R^2$ | RMSE | SEP | RPD |
| N | 0.67 | 0.03 | 0.03 | 1.79 | 3 | 0.60 | 0.04 | 0.04 | 1.52 |
| OM | 0.70 | 1.12 | 1.13 | 1.82 | 3 | 0.68 | 1.18 | 1.19 | 1.75 |
| Clay | 0.49 | 2.99 | 3.01 | 1.39 | 3 | 0.50 | 2.92 | 2.96 | 1.40 |
| Baseline normalization (BN) | | | | | | | | | |
| Variable | $R^2$ | RMSE | SEP | RPD | F | $R^2$ | RMSE | SEP | RPD |
| N | 0.64 | 0.04 | 0.04 | 1.75 | 2 | 0.59 | 0.04 | 0.04 | 1.54 |
| OM | 0.69 | 1.15 | 1.15 | 1.79 | 2 | 0.62 | 1.29 | 1.31 | 1.59 |
| Clay | 0.47 | 3.04 | 3.05 | 1.37 | 6 | 0.39 | 3.38 | 3.43 | 1.21 |
| First derivative (FD) | | | | | | | | | |
| Variable | $R^2$ | RMSE | SEP | RPD | F | $R^2$ | RMSE | SEP | RPD |
| N | 0.62 | 0.04 | 0.04 | 1.70 | 1 | 0.53 | 0.04 | 0.04 | 1.44 |
| OM | 0.67 | 1.18 | 1.18 | 1.74 | 2 | 0.66 | 1.22 | 1.23 | 1.69 |
| Clay | 0.37 | 3.33 | 3.35 | 1.25 | 4 | 0.64 | 2.54 | 2.58 | 1.61 |
| Standard normal variate (SNV) | | | | | | | | | |
| Variable | $R^2$ | RMSE | SEP | RPD | F | $R^2$ | RMSE | SEP | RPD |
| N | 0.62 | 0.04 | 0.04 | 1.707 | 2 | 0.54 | 0.04 | 0.04 | 1.47 |
| OM | 0.68 | 1.15 | 1.16 | 1.784 | 3 | 0.61 | 1.30 | 1.32 | 1.58 |
| Clay | 0.44 | 3.14 | 3.16 | 1.333 | 4 | 0.43 | 3.11 | 3.16 | 1.31 |
| Spectroscopy (SP) | | | | | | | | | |
| Variable | $R^2$ | RMSE | SEP | RPD | F | $R^2$ | RMSE | SEP | RPD |
| N | 0.69 | 0.03 | 0.03 | 1.892 | 1 | 0.61 | 0.04 | 0.04 | 1.54 |
| OM | 0.73 | 1.06 | 1.06 | 1.938 | 3 | 0.69 | 1.16 | 1.18 | 1.77 |
| Clay | 0.52 | 2.90 | 2.91 | 1.444 | 3 | 0.52 | 2.85 | 2.90 | 1.43 |
| Standard normal variate and detrending (SNV-D) | | | | | | | | | |
| Variable | $R^2$ | RMSE | SEP | RPD | F | $R^2$ | RMSE | SEP | RPD |
| N | 0.64 | 0.04 | 0.04 | 1.750 | 1 | 0.56 | 0.04 | 0.04 | 1.49 |
| OM | 0.70 | 1.13 | 1.13 | 1.821 | 2 | 0.62 | 1.28 | 1.30 | 1.61 |
| Clay | 0.39 | 3.26 | 3.28 | 1.283 | 7 | 0.54 | 2.93 | 2.98 | 1.39 |

$R^2$ (coefficient of determination); RMSE (root-mean-square error); RPD (residual prediction deviation); F (number of model factors).

The relationship of the predicted and measured data shows how the pre-processed SP (spectroscopy transformation) adjusted the data obtained in the laboratory with data captured by spectroscopy (all data) that presented good relationships (N: 0.69, OM: 0.73 and Clay: 0.52, Figure 5). The relationships between predicted and observed values have also shown good results with similar methodologies in work that studied the characterization of soils in different areas and determined nutrient cotton plants [58].

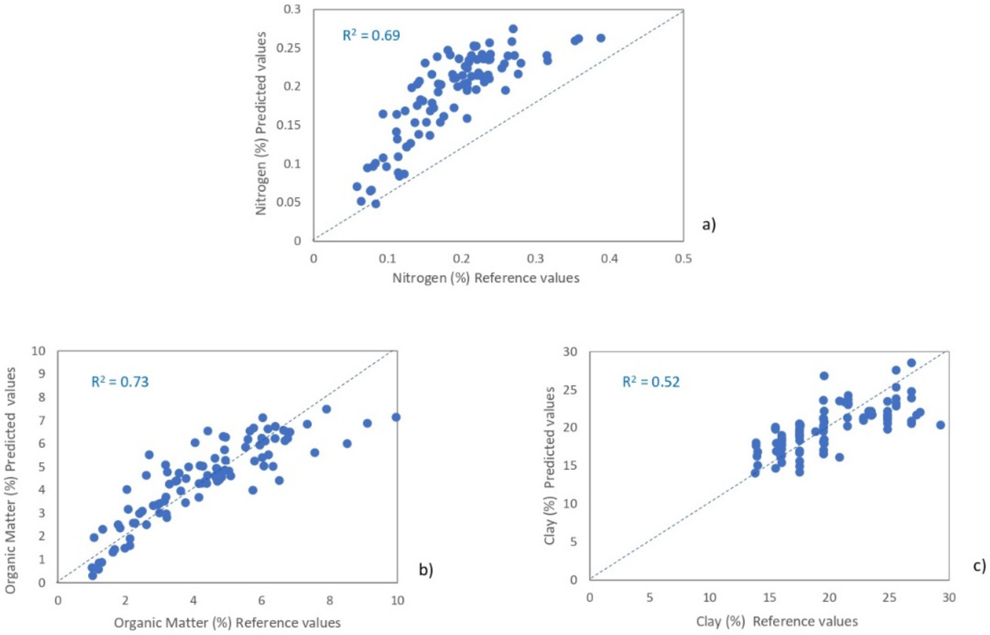

**Figure 5.** Relationship between predicted and reference values with the best pre-processing transformation (spectroscopy transformation SP and PLSR methodology) (**a**) Nitrogen, (**b**) Organic matter and (**c**) Clay.

### *3.4. Plot Mapping*

The spatial variability of soil elements in the vineyard allows us to offer a visualization of their spatial distribution and the change in the content throughout the seasons as a useful technique for vineyard management using spectroscopy.

Soil mapping of the vineyards under study has allowed us to observe the heterogeneous distribution of soil properties in the plot, more irregularly in the Lobeira vineyard (Figure 6), following a similar pattern in Monteveiga and Ribadulla plots regarding N content. The Lobeira plot was the vineyard with the middle content of N and OM; however, it had low clay content. In the Monteveiga and Ribadulla plots, the lowest contents of the variables studied were found in the border areas of the plot. Additionally, the similarity between maps analyzed with the different methodologies (laboratory analysis and PLSR with SP transformation) can be observed, which shows a good result in terms of the methodology defined in this work (Figure 6).

Comparisons of soil characterization in both methodologies were contrasted with the maps, in which it can be observed how the values do not exceed 7 % between both methodologies (Figure 7).

The results obtained by [59,60] in mapping elements for the characterization of the soil (C, clay and pH), captured using spectroscopy techniques and analyzed with the PLSR method, have been able to zone subareas with great heterogeneity among them, with very high $R^2$ values (0.92–0.93). The authors of [61] have also studied vineyards with differentiated subzones, with respect to the characterization of the vineyard soils, in this case, in relation with the topography parameters.

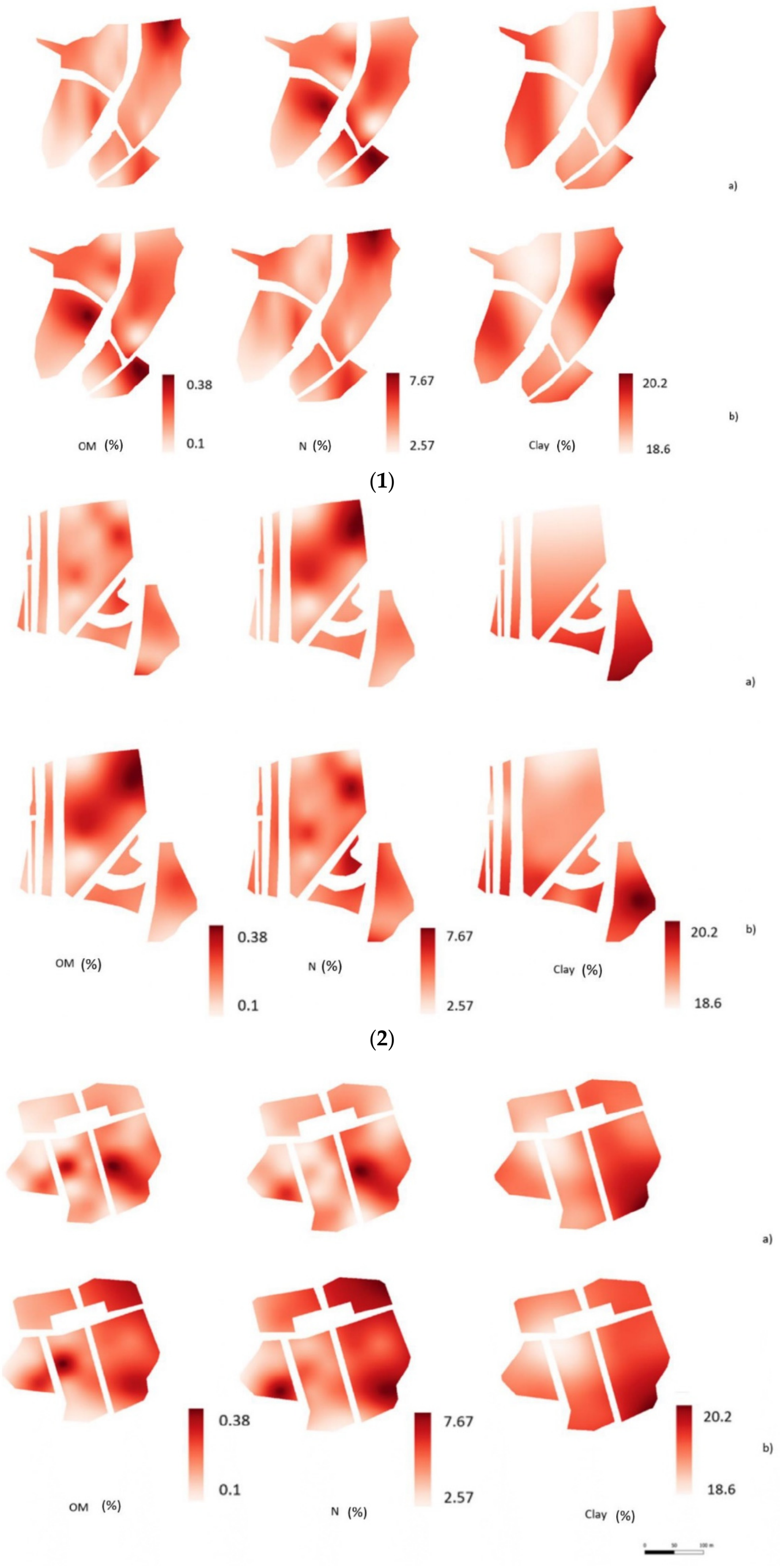

(**1**)

(**2**)

(**3**)

**Figure 6.** Mapping of variables to study (OM, N and clay) in Lobeira (**1**), Monteveiga (**2**) and Ribadulla (**3**) obtained from laboratory analysis data (**a**) and spectroscopy data (PLSR and spectroscopy transformation data) (**b**).

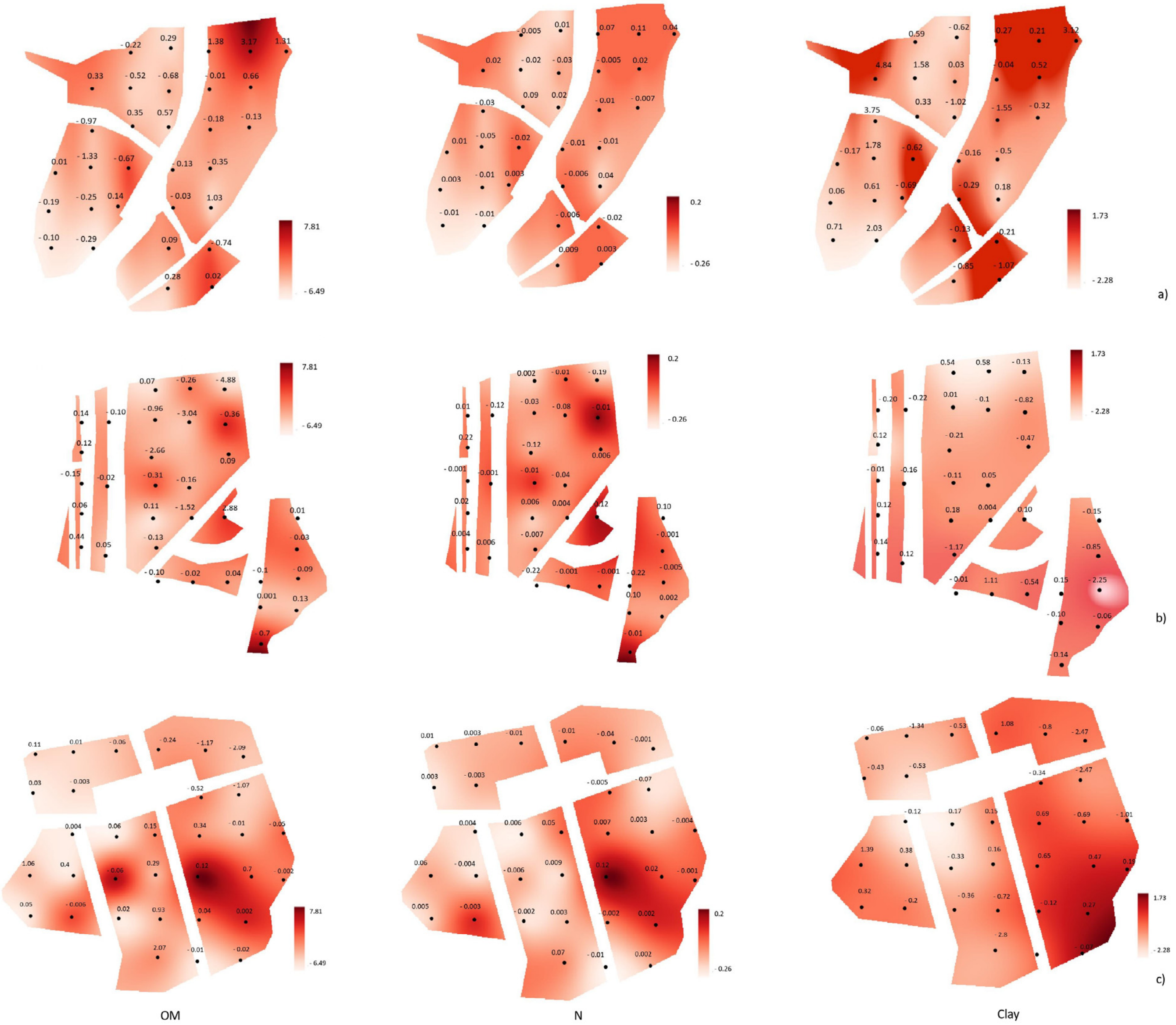

**Figure 7.** Difference (%) in OM, N and clay content, from the comparison of laboratory analysis and spectroscopy data; (**a**) Lobeira, (**b**) Monteveiga and (**c**) Ribadulla.

## 4. Conclusions

The characterization of the vineyard soil is a key piece of information that can contribute to better soil management. The conventional technique of soil fertility evaluation based on laboratory analysis is both time and cost consuming, and, hence, it is not suitable for precision agriculture. Thus, spectroscopy provides a complementary tool for soil characterization that is more efficient.

The methodology used determined precise data in the full spectral range, which is necessary for carrying out pre-processing. PLSR methodology has long been the method that presents the best results for data processing, with spectroscopy transformation (SP) obtaining the best prediction values of N and OM. One of the applications of soil characterization by spectroscopy is the mapping of the analyzed variables, which allows us to observe the distribution and characterization of the plot to be taken into account for good precision agricultural management.

However, the research line defined in the present work remains open to replication, in which the analysis of a greater number of samples, as well as more areas under study, corroborates the conclusions obtained regarding acidic soils. This approach allows us to visualize a future technique in which the improvement of data collection and processing helps to optimize this methodology measurement to be made directly in the vineyard.

**Author Contributions:** Conceptualization, M.R.-F., J.D., J.J.C. and J.R.R.-P.; methodology, M.R.-F., J.D. and J.R.R.-P.; software, M.R.-F. and J.R.R.-P.; validation, M.R.-F., J.D. and J.R.R.-P.; formal analysis, M.R.-F.; investigation, M.R.-F., M.F. and J.J.C.; resources, J.J.C. and J.R.R.-P.; data curation, M.R.-F. and J.D.; writing—original draft preparation, M.R.-F. and J.R.R.-P.; writing—review and editing, M.R.-F., J.D., M.F., J.J.C. and J.R.R.-P.; visualization, M.R.-F.; supervision, J.J.C.; project administration, J.J.C.; funding acquisition, J.J.C. All authors have read and agreed to the published version of the manuscript.

**Funding:** This work is a result of the Project: ALBASOUL-17 "Biotechnological strategies to optimize the management of Albariño varietal in the preparation of quiet and sparkling wines in the D.O. Rias Baixas—IDI-20180365" Mar de Frades Winery—Zamora Company, Vinesalt, financed by the program (Programa PID-CDTI) del Ministry of Economy Industry and Competitiveness.

**Acknowledgments:** To Consellería de Cultura, Educación e Universidade, Xunta de Galicia (Grupos de Referencia Competitiva ED431C-2021-27) and to the Edaphology Department of the University of Santiago de Compostela (EPSE-Lugo). Thanks to the anonymous reviewers for their comments and suggestions.

**Conflicts of Interest:** The authors declare no conflict of interest.

## References

1. Mashalaba, L.; Galleguillos, M.; Seguel, O.; Poblete-Olivares, J. Predicting Spatial Variability of Selected Soil Properties Using Digital Soil Mapping in a Rainfed Vineyard of Central Chile. *Geoderma Reg.* **2020**, *22*, e00289. [CrossRef]
2. Pouladi, N.; Møller, A.B.; Tabatabai, S.; Greve, M.H. Mapping soil organic matter contents at field level with Cubist, Random Forest and kriging. *Geoderma* **2019**, *342*, 85–92. [CrossRef]
3. Alfaia, S.S.; Ribeiro, G.A.; Nobre, A.D.; Luizão, R.C.; Luizão, F.J. Evaluation of soil fertility in smallholder agroforestry systems and pastures in western Amazonia. *Agric. Ecosyst. Environ.* **2004**, *102*, 409–414. [CrossRef]
4. Imre, S.P.; Kilmartin, P.A.; Rutan, T.; Mauk, J.L.; Nicolau, L. Influence of soil geochemistry on the chemical and aroma profiles of pinot noir wines. *J. Food Agric. Environ.* **2012**, *10*, 280–288.
5. Tajik, S.; Ayoubi, S.; Zeraatpisheh, M. Digital mapping of soil organic carbon using ensemble learning model in Mollisols of Hyrcanian forests, northern Iran. *Geoderma Reg.* **2020**, *20*, e00256. [CrossRef]
6. Brevik, E.C.; Calzolari, C.; Miller, B.A.; Pereira, P.; Kabala, C.; Baumgarten, A. Soil mapping, classification, and pedologic modeling: History and future directions. *Geoderma* **2016**, *264*, 256–274. [CrossRef]
7. Fathololoumi, S.; Vaezi, A.R.; Alavipanah, S.K.; Ghorbani, A.; Saurette, D.; Biswas, A. Improved digital soil mapping with multitemporal remotely sensed satellite data fusion: A case study in Iran. *Sci. Total Environ.* **2020**, *721*, 137703. [CrossRef]
8. Xing, Z.; Tian, K.; Du, C.; Li, C.; Zhou, J.; Chen, Z. Agricultural soil characterization by FTIR spectroscopy at micrometer scales: Depth profiling by photoacoustic spectroscopy. *Geoderma* **2019**, *335*, 94–103. [CrossRef]
9. Van der Meer, F. The effectiveness of spectral similarity measures for the analysis of hyperspectral imagery. *Int. J. Appl. Earth Obs. Geoinf.* **2006**, *8*, 3–17. [CrossRef]
10. Tian, Y.; Zhang, J.; Yao, X.; Cao, W.; Zhu, Y. Laboratory assessment of three quantitative methods for estimating the organic matter content of soils in China based on visible/near-infrared reflectance spectra. *Geoderma* **2013**, *202–203*, 161–170. [CrossRef]
11. Cambule, A.H.; Rossiter, D.G.; Stoorvogel, J.J.; Smaling, E.M.A. Building a near infrared spectral library Journal of Spectroscopy 11 for soil organic carbon estimation in the Limpopo national park, Mozambique. *Geoderma* **2012**, *183–184*, 41–48. [CrossRef]
12. Bowers, S.; Hanks, R.J. Reflectance of radiant energy from soils. *Soil Sci.* **1965**, *100*, 130–138. [CrossRef]
13. Dalal, R.C.; Henry, R.J. Simultaneous determination of moisture, organic carbon, and total nitrogen by near infrared reflectance spectrophotometry. *Soil Sci. Soc. Am. J.* **1986**, *50*, 120–123. [CrossRef]
14. Ben-Dor, E. Quantitative remote sensing of soil properties. In *Advances in Agronomy*; Academic Press: Cambridge, MA, USA, 2002; Volume 75, pp. 173–243.
15. Hill, J.; Schütt, B. Mapping complex patterns of erosion and stability in dry Mediterranean ecosystems. *Remote Sens. Environ.* **2000**, *74*, 557–569. [CrossRef]
16. Demattê, J.A.; Campos, R.C.; Alves, M.C.; Fiorio, P.R.; Nanni, M.R. Visible-NIR reflectance: A new approach on soil evaluation. *Geoderma* **2004**, *121*, 95–112. [CrossRef]
17. Nanni, M.R.; Demattê, J.A.M.; Fiorio, P.R. Discriminant analysis two alone by means of non-terrestrial level spectral response. *Pesq. Agropec. Bras.* **2004**, *39*, 995–1006. [CrossRef]
18. Seema; Ghosh, A.K.; Das, B.S.; Reddy, N. Application of VIS-NIR spectroscopy for estimation of soil organic carbon using different spectral preprocessing techniques and multivariate methods in the middle Indo-Gangetic plains of India. *Geoderma Reg.* **2020**, *23*, e00349. [CrossRef]

19. Tan, K.H. *Soil Sampling, Preparation and Analysis*; Marcel Dekker: New York, NY, USA, 1996.
20. Comino, J.R.; Bogunovic, I.; Mohajerani, H.; Pereira, P.; Cerdà, A.; Ruiz Sinoga, J.D.; Ries, J.B. The impact of vineyards abandonment on soil properties and hydrological processes. *Vadose Zone J.* **2017**, *16*, 1–7. [CrossRef]
21. Peregrina, F.; Pérez-Álvarez, E.P.; Colina, M.; García-Escudero, E. Cover crops and tillage influence soil organic matter and nitrogen availability in a semi-arid vineyard. *Arch. Agron. Soil Sci.* **2012**, *58*, SS95–SS102. [CrossRef]
22. Boyoucos, G.F. Hidrometer method improved for making particle size analyses of soils 1. *Agron. J.* **1962**, *54*, 464–465. [CrossRef]
23. Fernández, I.; Cabaneiro, A.; Carballas, T. Organic matter changes immediately after a wildfire in an Atlantic forest soil and comparison with laboratory soil heating. *Soil Biol. Biochem.* **1997**, *29*, 1–11. [CrossRef]
24. Vašát, R.; Kodešová, R.; Klement, A.; Borůvka, L. Simple but efficient signal pre-processing in soil organic carbon spectroscopic estimation. *Geoderma* **2017**, *298*, 46–53. [CrossRef]
25. Rinnan, Å.; Van Den Berg, F.; Engelsen, S.B. Review of the most common pre-processing techniques for near-infrared spectra. *TrAC Trends Anal. Chem.* **2009**, *28*, 1201–1222. [CrossRef]
26. Buddenbaum, H.; Steffens, M. The effects of spectral pretreatments on chemometric analyses of soil profiles using laboratory imaging spectroscopy. *Appl. Environ. Soil Sci.* **2012**, *2012*, 274903. [CrossRef]
27. McBratney, A.B.; Minasny, B.; Rossel, R.V. Spectral soil analysis and inference systems: A powerful combination for solving the soil data crisis. *Geoderma* **2006**, *136*, 272–278. [CrossRef]
28. Williams, P.; Dardenne, P.; Flinn, P. Tutorial: Items to be included in a report on a near infrared spectroscopy project. *J. Near Infrared Spectrosc.* **2017**, *25*, 85–90. [CrossRef]
29. Næs, T.; Isaksson, T.; Fearn, T.; Davies, T. *A User-Friendly Guide to Multivariate Calibration and Classification*; NIR Publications: Chichester, UK, 2002; Volume 6.
30. Cozzolino, D.; Cynkar, W.U.; Dambergs, R.G.; Shah, N.; Smith, P. In situ measurement of soil chemical composition by near-infrared spectroscopy: A tool toward sustainable vineyard management. *Commun. Soil Sci. Plant Anal.* **2013**, *44*, 1610–1619. [CrossRef]
31. Breiman, L. Random forests. *Mach. Learn.* **2001**, *45*, 5–32. [CrossRef]
32. Goydaragh, M.G.; Taghizadeh-Mehrjardi, R.; Jafarzadeh, A.A.; Triantafilis, J.; Lado, M. Using environmental variables and Fourier Transform Infrared Spectroscopy to predict soil organic carbon. *Catena* **2021**, *202*, 105280. [CrossRef]
33. Houborg, R.; McCabe, M.F. A hybrid training approach for leaf area index estimation via Cubist and random forests machine-learning. *ISPRS J. Photogramm. Remote Sens.* **2018**, *135*, 173–188. [CrossRef]
34. Liaw, A.; Wiener, M. Classification and regression by randomForest. *R News* **2002**, *2*, 18–22.
35. Bellon-Maurel, V.; Fernandez-Ahumada, E.; Palagos, B.; Roger, J.-M.; McBratney, A. Critical review of chemometric indicators commonly used for assessing the quality of the prediction of soil attributes by NIR spectroscopy. *TrAC Trends Anal. Chem.* **2010**, *29*, 1073–1081. [CrossRef]
36. Lu, P.; Wang, L.; Niu, Z.; Li, L.; Zhang, W. Prediction of soil properties using laboratory VIS–NIR spectroscopy and Hyperion imagery. *J. Geochem. Explor.* **2013**, *132*, 26–33. [CrossRef]
37. Vasques, G.M.; Grunwald, S.; Sickman, J.O. Comparison of multivariate methods for inferential modeling of soil carbon using visible/near-infrared spectra. *Geoderma* **2008**, *146*, 14–25. [CrossRef]
38. Rossiter, D.G. Applied Geostatistics Tutorial: Regional Mapping of Climate Variables from Point Simples. 2019. Available online: http://www.css.cornell.edu/faculty/dgr2/_static/files/R_PDF/exRKGLS.pdf (accessed on 9 November 2021).
39. Nychka, D.; Furrer, R.; Paige, J.; Sain, S. "Fields: Tools for Spatial Data". R Package Version 13.3. 2021. Available online: https://github.com/dnychka/fieldsRPackage (accessed on 2 January 2022).
40. Rossiter, D.G. Exercise: Thin Plate Spline Interpolation. Cornell University. 2016. Available online: http://www.css.cornell.edu/faculty/dgr2/_static/files/R_PDF/exTPS.pdf (accessed on 9 November 2021).
41. Rossel, R.V.; McBratney, A.B. Diffuse reflectance spectroscopy as a tool for digital soil mapping. In *Digital Soil Mapping with Limited Data*; Springer: Dordrecht, The Netherlands, 2008; pp. 165–172.
42. Wetterlind, J.; Stenberg, B.; Söderström, M. The use of near infrared (NIR) spectroscopy to improve soil mapping at the farm scale. *Precis. Agric.* **2008**, *9*, 57–69. [CrossRef]
43. Stenberg, B.; Rossel, R.A.V.; Mouazen, A.M.; Wetterlind, J. Visible and near infrared spectroscopy in soil science. *Adv. Agron.* **2010**, *107*, 163–215.
44. Jarquin-Sanchez, A.; Salgado-Garcia, S.; Palma-López, D.J.; Camacho-Chiu, W.; Guerrero-Pena, A. Analysis of total nitrogen in tropical soils with near-infrared spectroscopy (NIRS) and chemometrics. *Agrociencia* **2011**, *45*, 653–662.
45. Northup, B.K.; Daniel, J.A. Near Infrared Reflectance-Based Tools for Predicting Soil Chemical Properties of Oklahoma Grazing-lands. *Agron. J.* **2012**, *104*, 1122–1129. [CrossRef]
46. Chang, C.-W.; Laird, D.; Mausbach, M.J.; Hurburgh, C.R., Jr. Near-infrared reflectance spectroscopy–principal components regression analyses of soil properties. *Soil Sci. Soc. Am. J.* **2001**, *65*, 480. [CrossRef]
47. Gras, J.-P.; Barthès, B.G.; Mahaut, B.; Trupin, S. Best practices for obtaining and processing field visible and near infrared (VNIR) spectra of topsoils. *Geoderma* **2014**, *214*, 126–134. [CrossRef]
48. Bonett, J.P.; Camacho-Tamayo, J.H.; Ramírez-López, L. Mid-infrared spectroscopy for the estimation of some soil properties. *Agron. Colomb.* **2015**, *33*, 99–106. [CrossRef]

49. Perret, J.; Villalobos-Leandro, J.E.; Abdalla-Bolaños, K.; Fuentes-Fallas, C.L.; Cuarezma-Espinoza, K.M.; Macas-Amaya, E.N.; López-Maietta, M.T.; Drewry, D. Development of spectroscopic methods and machine learning algorithms for evaluation of some soil properties in Costa Rica. *Agron. Costarric.* **2020**, *44*, 139–154.
50. Zhao, D.; Arshad, M.; Wang, J.; Triantafilis, J. Soil exchangeable cations estimation using Vis-NIR spectroscopy in different depths: Effects of multiple calibration models and spiking. *Comput. Electron. Agric.* **2021**, *182*, 105990. [CrossRef]
51. Ball, K.R.; Baldock, J.A.; Penfold, C.; Power, S.A.; Woodin, S.J.; Smith, P.; Pendall, E. Soil organic carbon and nitrogen pools are increased by mixed grass and legume cover crops in vineyard agroecosystems: Detecting short-term management effects using infrared spectroscopy. *Geoderma* **2020**, *379*, 114619. [CrossRef]
52. Viscarra Rossel, R.; McBratney, A.; Minasny, B. *Proximal Soil Sensing*; Springer: Dordrecht, The Netherlands, 2010.
53. Ben-Dor, E.; Banin, A. Near-infrared analysis as a rapid method to simultaneously evaluate several soil properties. *Soil Sci. Soc. Am. J.* **1995**, *59*, 364–372. [CrossRef]
54. Udelhoven, T.; Emmerling, C.; Jarmer, T. Quantitative analysis of soil chemical properties with diffuse reflectance spectrometry and partial least-square regression: A feasibility study. *Plant Soil* **2003**, *251*, 319–329. [CrossRef]
55. Kooistra, L.; Wehrens, R.; Leuven, R.; Buydens, L.M.C. Possibilities of visible–near-infrared spectroscopy for the assessment of soil contamination in river floodplains. *Anal. Chim. Acta* **2001**, *446*, 97–105. [CrossRef]
56. Du, C.; Zhou, J. Evaluation of Soil Fertility Using Infrared Spectroscopy—A Review. In *Climate Change, Intercropping, Pest Control and Beneficial Microorganisms*; Springer: Dodrecht, The Netherlands, 2009; pp. 453–483.
57. Mukrimin, M.; Conrad, A.O.; Kovalchuk, A.; Julkunen-Tiitto, R.; Bonello, P.; Asiegbu, F.O. Fourier-transform infrared (FT-IR) spectroscopy analysis discriminates asymptomatic and symptomatic Norway spruce trees. *Plant Sci.* **2019**, *289*, 110247. [CrossRef]
58. Rosero-Vlasova, O.A.; Pérez-Cabello, F.; Llovería, R.M.; Vlassova, L. Assessment of laboratory VIS-NIR-SWIR setups with different spectroscopy accessories for characterisation of soils from wildfire burns. *Biosyst. Eng.* **2016**, *152*, 51–67. [CrossRef]
59. Odlare, M.; Svensson, K.; Pell, M. Near infrared reflectance spectroscopy for assessment of spatial soil variation in an agricultural field. *Geoderma* **2005**, *126*, 193–202. [CrossRef]
60. He, Y.; Song, H.; Pereira, A.G.; Gómez, A.H. A new approach to predict N, P, K and OM content in a loamy mixed soil by using near infrared reflectance spectroscopy. In Proceedings of the International Conference on Intelligent Computing, Hefei, China, 23–26 August 2005; pp. 859–867.
61. Vadillo, J.A.; Izquierdo, L.M.O.; Flaño, P.R.; Martínez, T.L. Spatial distribution of the vineyard in the autonomous community of La Rioja: Influence of topography and landforms. *Polígonos Rev. Geogr.* **2006**, *16*, 11–34.